Modeling a Novel Shallow Ground Heat Exchanger

Michele Bottarelli*[1], Marco Bortoloni[1]
[1]Università degli Studi di Ferrara, Dipartimento di Architettura, Ferrara, Italia
*Corresponding author: via Quartieri, 8 – 44121 Ferrara; michele.bottarelli@unife.it

Abstract: This paper presents the implementation of the numerical model COMSOL Multiphysics to analyze the behaviour of a novel shallow ground heat exchanger, named flat panel, whose shape is similar to a plate installed edgeways in a shallow trench. A three-dimensional domain with hourly time-varying boundary conditions at the ground surface and at the closed loop was implemented to evaluate the energy performance and the thermal field of the surrounding soil. The model was run for a full year, simulating the heating and cooling load of a hypothetical building, as related with the climate in Northern Italy.

The results show that the maximum specific power initially supposed for the flat panel (40 W/m), as concluded in a different study, can be increase for the supposed environmental conditions, when a labyrinth is made inside the hollow. Moreover, unlike with the vertical deep exchangers, the flat panel highlights that long-term subsurface thermal energy build-up or depletion should be not expected by shallow exchangers, because the solar energy balance on soil surface is higher than the rate exchanged between ground and exchanger.

Keywords: horizontal ground heat exchanger, flat panel, three-dimensional domain, unsteady state analysis.

1. Introduction

Ground heat exchangers (GHEs) are rarely installed horizontally in linked ground source heat pumps used for space conditioning, because their energetic performance is lower than in the vertical solution. However, the horizontal one holds several advantages: it is easy to carry out and upkeep, more compliant with environmental regulations, and interferes marginally with groundwater systems. Moreover, the seasonal heat transfer over the soil surface resets the memory of the energy exploitation carried out by a GHE, because the shallow energy balance depends larger on the solar energy than on the deep geothermal source. This reflects the main difference to the vertical GHEs, whose performance is linked to a balance in heating and cooling requirements close to zero.

To preserve these advantages and improve the energetic performance, we have examined a novel geometry for horizontal ground heat exchanger (HGHE), consisting in a flat panel (FP) installed edgeways into a trench at shallow depth, and virtually coupled with a heat pump for heating and cooling. The present 3D numerical approach is similar to [1,2], where the behavior of the FP is evaluated by means of the FEFLOW model, an unsteady-state 3D numerical finite element code solving the groundwater flow and heat transfer in porous media.

2. Methodology

COMSOL Multiphysics is here implemented to model a 3D domain with hourly time-varying boundary conditions supposed at the ground surface and closed loop. The 3D approach is chose to analyze the temperature variation into the exchanger, unlike the approach in [3], where a 2D cross section is taken in account to solve the exchange for unit meter of exchanger.

Hourly heat loads due to heat pump operation are modeled as transient heat fluxes imposed on the closed loop inlet/outlet. The heat loads are assessed linking the energy requirements to the outdoor air temperature time series, and simplifying the building as a homogenous lumped system, whose internal energy variation occurs due to the heat transfer through its envelope.

2.1 Model Domain

The computational domain geometry and parameters follow from the general layout of the HGHE and its construction technology.

The reference case consists in a FP surrounded by a ground volume 12 m long, 9 m wide and 8 m deep. Preliminary simulations carried out with a shallower domain showed that the GHE activity is able to modify slightly the temperature beyond similar depth.

For simplicity, the symmetric approach is

considered, and the FP represents the symmetric line, to halve the domain and reduce the finite elements (Fig. 1). The FP occupies the full length of the domain (12m), to express the behaviour of a part of a longer exchanger. Its cross-section is represented in the model by a rectangle 100x3 cm. Here, the presence of the panel wall (and its thermal resistance) is neglected, and the fluid is pure water.
The FP is supposed installed between 1 m and 2 m deep in soil, taken to be horizontal in the entire domain, typically for shallow HGHEs.
The domain was considered as a homogeneous virtual solid soil, without taking into account any flow field in porous media. Its properties (x_{domain}) become as weighted average by means of solid (x_{solid}) and water (x_{liquid}) properties, assuming a porosity (n) of 37%:

$$x_{domain} = n \cdot x_{liquid} + (1-n) \cdot x_{solid} \quad (1)$$

The hydraulic and thermal properties attributed to the different materials constituting the domains (fluid and soil) are summarized in Table 1.
The final mesh is composed by 164,000 finite elements; a higher concentration of elements was imposed within and around the fluid domain to represent more accurately the difference in the hydraulic and thermal properties of the pipe and the surrounding soil. Further, a boundary-layer has been used on the panel wall. Finally, edges and boundaries of domains were managed in order to make the mesh as homogeneous as possible. The mesh adopted for the simulation showed to be sufficient to achieve the convergence of the results. For simplicity sensitivity analysis has not been inserted here.
In four slices are located 19 observation points, to measure the thermal field from top to bottom of the domain, and at several distances from the FP (15, 50, 100, 300 cm). Furthermore, to detect the temperatures of inlets and outlets, other two observation points was positioned at the FP in/out.

	Solid	*Liquid*	*Domain*	
Thermal conductivity	2.20	0.65	1.63	*W/m K*
Density	2500	1000	1700	*kg/m³*
Specific heat	900	4200	1600	*J/kg K*
Porosity	-	-	0.37	*1*

Table 1. Thermal properties

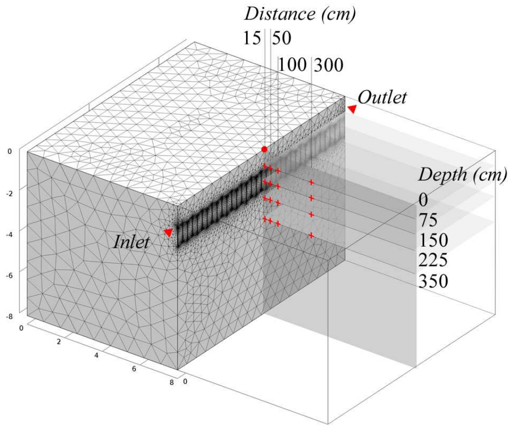

Figure 1. Computational mesh and observation points

2.2 Boundary Conditions

Boundary conditions of the 1st and 2nd kind were fixed at the outer domain boundaries and within the FP, as hydraulic and thermal conditions.
A heat flux density time series was assigned as thermal boundary condition on the soil surface. The time series represents the net solar energy deepening in soil. The data results from the study reported in [1] and [2], where a different CFD model (FEFLOW) was implemented in a similar domain, characterized with identical material properties. In that case, the model was run for a whole year with an imposed temperature time series over the soil surface, to obtain indirectly the previous hourly heat flux, which is presented in Fig. 2. In this figure, the values are included in the interval ±100 W/m^2, and the corresponding cumulative energy balance oscillates between ±20 kWh/m^2 per year. Similar data are reported in [4], where it is specified that the surface soil heat flux typically varies within 1 to 10% of the net solar radiation. The resulting time series is imported in COMSOL directly from an external text file, compiled with 8760 values.
To define the hourly heat power at the FP, the methodology reported in [1] is applied, where the energy requirement of a hypothetical building is essentially linked to the previous air temperature time series. The building is simplified in a lumped system, and its energy variation occurs owing to the heat transfer through its envelope. The degree-days result almost 2600 in heating mode, and 400 in cooling. The system is supposed operating in heating mode from October 15th to April 30th and

in cooling mode from June 1st to September 30th. Its activity hours are selected to be representative of typical working conditions at the residential scale: 5 AM - 9 AM and 5 PM - 10 PM from Monday to Friday, 7 AM - 11 PM on the weekends.
To relate the former energy requirements to the FP, a constant water mass flow rate is assumed (3.5 m^3/d), and a difference of temperature is calculated to express the heat power needed. The resulting time series was imported in COMSOL via an external text file; then, an expression is implemented for applying this difference at the FP outlet temperature to define the inlet temperature. This method resolves the operation carried out from the heat pump, which drops or raises the FP water leaving temperature.
At the bottom of the domain, the temperature is always fixed equal to 16°C, representing an undisturbed condition similar at the average value of the air temperature.
All boundary conditions are representative of average conditions in northern Italy.
The soil initial temperature field was obtained by means of a preliminary modeling in absence of the FP activity. To do so, a simulation was carried out for a full year, starting from an uniform initial soil temperature of 16°C.

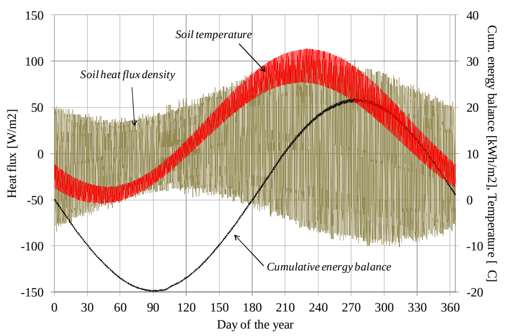

Figure 2. Heat flux density, cumulative energy balance and soil temperature

2.3 Initial conditions

A preliminary fluid-dynamics simulation was carried out to solve the velocity field in the fluid domain, assuming laminar flow and steady state conditions (Fig. 3)**.** For simplicity, the laminar approach was supposed, also supported by the resulting Reynold's number inside the rectangular channel of the FP (*Re≤ 1000*). Nevertheless, the meanderings shown in Fig. 3 could express local turbulences; so, we will applied the turbulence approach in the next future, together with a boundary condition on the soil surface of the 3rd kind, in alternative of heat flux.
The thermal analysis was performed starting from an constant initial distribution of temperature set to 16 °C, in absence of the FP activity, and given the former velocity field.
The model run for 365 day, and the initial condition for thermal field was assumed that resulting at October, 15th, which represents the beginning of the heating season in Italy.

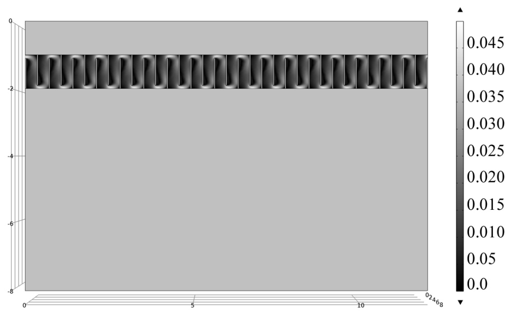

Figure 3. Velocity field resulting from CFD module in steady state, (m/s)

3. Results

The thermal analysis was solved for a total of 36.500 degrees of freedom. The simulation time for a full year was completed in about 5 hours using an Intel(R) Core(TM) i7 with 6 CPU, and 16GB RAM memory.
The model was run for 365 days starting from October, 15th, to obtain the time-varying thermal field within the FP and the soil, during the wintertime and summertime. The following results are shown as temperature time series at several observation points and at FP inlet/outlet (Figs. 4-9), and as textured pictures for two sections of the domain (Fig. 10 and 11).
In detail, Fig. 4 depicts the daily average water temperature at the FP inlet and outlet (T_inlet^, T_outlet^), and at three points located 100 cm far from the FP and 150, 225 and 350 cm deep in soil, (150_100^, 225_100^, 350_100^), together with the reference point in the middle of the soil surface (0_0), which is in absence of the FP activity. Fig. 5 retails the hourly FP operation during a whole week; here, the higher employment during the week-end is well

highlighted from the two wider areas. Taking into account both the previous pictures, the FP shows a thermal recover never less than 2°C, equivalent to an average specific power always over 25 W/m, a maximum one of 40 W/m, and an overall energy exchanged of +90/-10 kWh/m*y in winter/summer. Since the inlet temperature never drops beyond 4°C, it would be possible to force the FP performance for reaching lower temperature. It expresses that a higher specific power has to be expected from the FP in similar environmental conditions. Identical power data were obtained in [2], but the resulting minimum temperature was 0°C. The difference should be related to the labyrinth inserted in the present analysis, which didn't introduced in the FP implemented in [2].

From Fig. 6 to Fig. 9, the temperature time series are presented for four points located at equivalent distance from the FP (15, 50, 100, 300 cm), and for different depths from soil surface (75, 150, 225, 350 cm). The temperature of the case without the FP is always included to estimate directly the FP impact. In these figures, the difference between the initial and final temperatures has to be related to a non-zero energy balance of the system. Although the heat flux imposed over the soil surface assumes a yearly zero energy balance, what is yearly exchanged from the FP defines an overall negative balance in the domain.

In Fig. 7, the temperature time series of the undisturbed point 150_15 is very close to that of the equivalent point 300 cm far from the FP (150_300^). It expresses that the impact of the FP don't reach farther distance. Moreover, all the figure shows that the most intense FP impact performed in wintertime is recovered quickly and before the summertime. This remark can be also express by Fig. 8 and 9.

Finally, in Fig. 10, 11 and 12 are presented two section of the domain and a 3D picture of the thermal field at 444.5 day of the year. This time represents a harder moment for the system, because it is late in winter and during a week-end, shown in Fig. 5.

The side section in Fig. 10 shows how the soil heats the water into the exchanger, and how works the labyrinth. In Fig. 11, the cross section shows how the FP impact onto the soil; over the exchanger is well highlighted the lowest temperature, and the major drop reaches up to 2 m transversally from the FP.

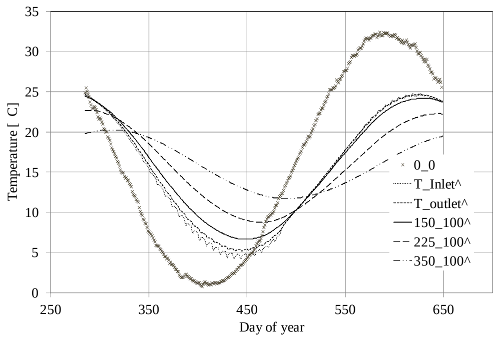

Figure 4. Observation points at 100 cm from the FP

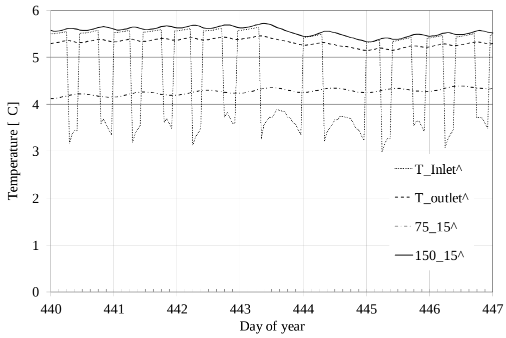

Figure 5. Operating weekly detail

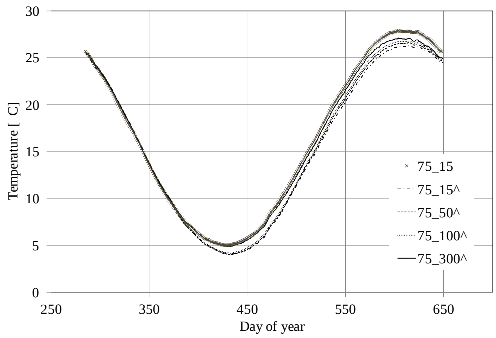

Figure 6. Observation points at 75 cm deep in soil

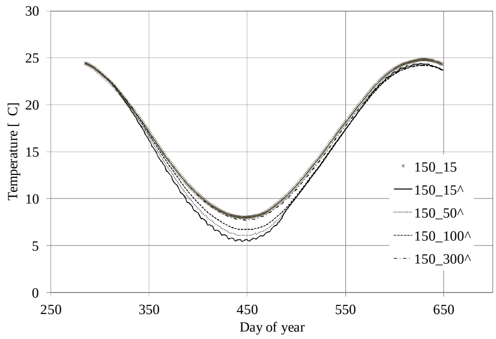

Figure 7. Observation points at 150 cm deep in soil

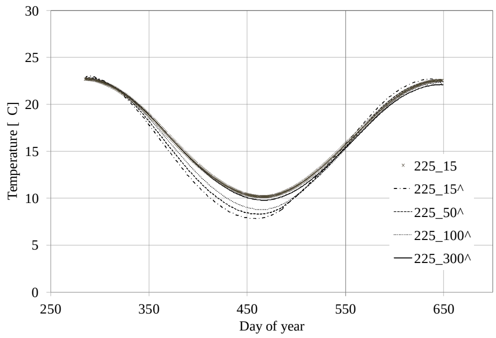

Figure 8. Observation points at 225 cm deep in soil

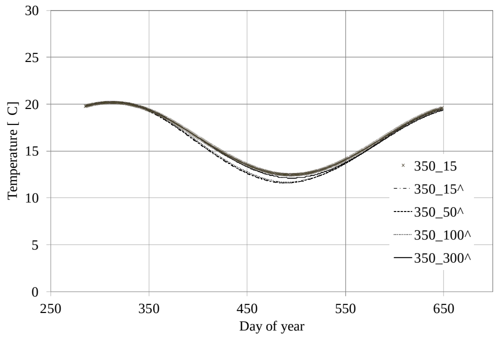

Figure 9. Observation points at 350 cm deep in soil

4. Conclusions

An analysis of heat transport induced in the ground by the presence of a shallow horizontal ground heat exchanger (HGHE) was presented, adopting a flat panel shape (FP) to improve the energetic performance of the horizontal installation.
Hourly heat loads are modeled as transient heat fluxes imposed at the inlet of the closed loop, to reproduce the energy requirements of hypothetical building, whose internal energy variation occurs due to the heat transfer through its envelope. The energy balance over the soil surface is introduced as hourly heat flux density at the top of the domain, to represent the net solar energy deepening the soil.
The study was conducted via the implementation of an unsteady-state three-dimensional numerical finite element model, considering the HGHE and the surrounding soil as an unique system. The model implemented was COMSOL Multiphysics, which showed a wide versatility and high performance in controlling so long time simulation.
The result show that the specific power initially supposed for the FP (40 W/m), as assumed from a former study, could be increase in similar environmental conditions, because the minimum temperature reached in wintertime was 4°C. Since no differences were introduced in this model in comparison with the former one, with the exception of the numerical model (FEFLOW) and the absence of the labyrinth here supposed inside the FP hollow, we deem that the higher performance could be related to the labyrinth.
Moreover, unlike with the vertical deep exchangers, the FP behaviour highlights that long-term subsurface thermal energy build-up or depletion would not be expecting by shallow HGHEs.

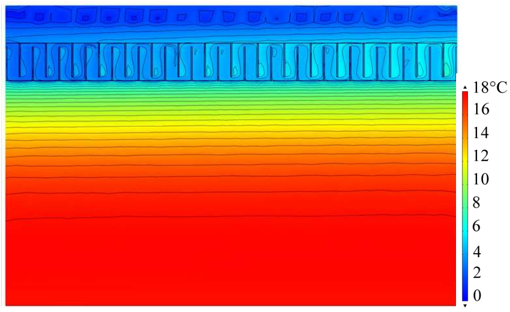

Figure 10. Side section; thermal filed at 444.5 DOY

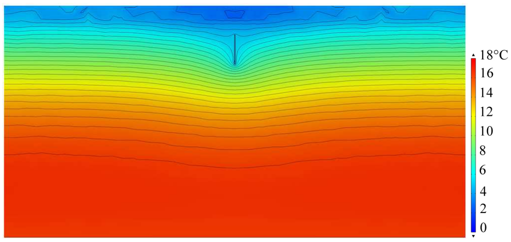

Figure 11. Cross section; thermal filed at 444.5 DOY

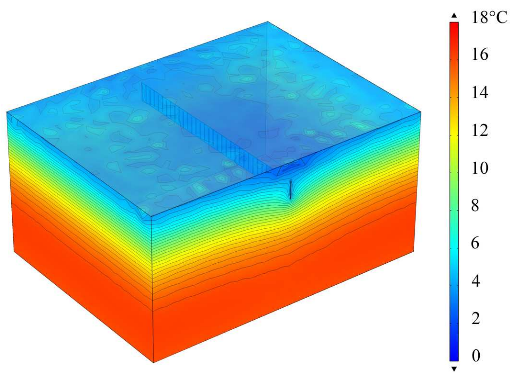

Figure 12. 3D thermal field at 444.5 DOY

5. References

1. Bottarelli M. Gabrielli L., Payback period for a ground source heat pump system, Int. Journal of Heat & Technology, vol. 29/2, Pp. 145-150 (2011)

2. Bottarelli M., Di Federico V., Numerical comparison between two advanced HGHEs, Int. Journal of Low-Carbon Technologies, vol. 7/2, Pp. 75-81 (2012)

3. A. D. Chiasson, Modeling Horizontal Ground Heat Exchangers in Geothermal Heat Pump Systems, Proceedings of COMSOL conference (2010)

4. T.J. Sauer, R. Horton, Micrometeorology in agricultural systems, vol. 47, Pp. 131-154 (2005)